

**Comparisons of Slip-Corrected Reynolds Lubrication
Equations for the Air Bearing Film in the Head-Disk Interface
of Hard Disk Drives**

Du Chen and David B. Bogy

Computer Mechanics Laboratory

Dept. of Mechanical Engineering

University of California

Berkeley, CA 94720

ABSTRACT

Slip-corrected Reynolds equations have not been widely used in the data storage air bearing simulations since Fukui and Kaneko [1] published a more accurate generalized lubrication equation (FK model) based on the linearized Boltzmann equation for the molecular gas lubrication. Recently some new slip models and slip-corrected Reynolds equations have been proposed with certain improvements or a kinetic theory basis. This report reanalyzes those slip models and lubrication equations developed after the FK model was published. It is found that all of the slip-corrected Reynolds equations are of limited use in the simulation of molecular gas lubrication, and that these new slip-corrected Reynolds equations can not replace the FK model in the air bearing simulation.

1. Introduction

Slip-corrected Reynolds lubrication equations are important in the modeling of the low subsonic air bearing film in the head disk interface of hard disk drives. The classical compressible Reynolds lubrication equation is derived from the Navier-Stokes equation with the continuum no-slip boundary condition. It is not accurate when the gas rarefaction comes into effect, as happens when the slider to disk spacing is substantially less than the mean free path of the ambient gas molecules. In the past as the slider-disk gap was reduced from microns to nanometers, the velocity slip was taken into consideration. However, slip-corrected Reynolds equations have not been widely used in the air bearing simulations since Fukui and Kaneko [1] derived a more accurate generalized lubrication equation (FK model) based on the linearized Boltzmann equation with the Bhatnager-Gross-Krook (BGK) model [2]. The slip-corrected Reynolds equations may not be valid for ultra-thin air bearing films with local transition flows or free molecular flows, due to the limitation of the slip flow models. Contrarily, the FK lubrication equation, which has a similar form to that of slip-corrected Reynolds lubrication equations, is valid for arbitrary Knudsen numbers.

A slip-corrected Reynolds lubrication equation is based on a slip model of the velocity boundary condition. The first-order slip model, which was originally developed by Maxwell [3], was incorporated into the Reynolds equation by Burgdorfer [5]. Hsia and Domoto [6] derived a second-order slip model using a Taylor expansion of the bulk mean velocity and obtained a new Reynolds equation. Mitsuya [7] developed a kinetic-theory

based so-called “1.5-order” slip model and modified the Reynolds equation accordingly. Recently Wu and Bogy derived a pressure gradient model [8] and new first- and second-order slip models [9] from a more physical point of view. Hwang [10] and Ng et. al. [11 and 12] obtained different slip models using a mathematical interpolation of the numerical results of the linearized Boltzmann equation or the DSMC method, respectively. Shen and Chen [13] analyzed the linearized Boltzmann equation with the BGK model for Poiseuille flow and derived a “first-order” slip model. Peng et. al. [14] modified the gas molecule’s mean free path due to the existence of boundaries of the air bearing film and applied this modification to different slip models and the corresponding Reynolds equations. Bahukudumbi and Beskok [15] obtained a Reynolds equation valid in a wide range of Knudsen numbers, using a modified slip boundary condition for steady plane Couette flows [16] and a generalized higher-order slip model for pressure-driven flows [17].

All of these efforts on slip-corrected Reynolds equations uncover certain physical aspects of rarefaction effects on an air bearing; however, they do not show any important advantages over the generalized Reynolds equation derived by Fukui and Kaneko [1], except for Wu’s work [8] and Peng’s modification of the mean free path [14]. Wu showed that, unlike the FK model, the 1.5- and second-order slip-corrected Reynolds equations do not have the unbounded air pressure singularities when the air bearing is at or near contact. Peng et. al. [14] applied the gas molecule’s modified mean free path to the FK model and changed the Poiseuille flow rate coefficient in the molecular gas lubrication

equation.

The question arises as to whether or not these improvements should be incorporated into the numerical simulation of the air bearing film in a head disk interface. This report reanalyzes these slip models and the corresponding slip-corrected Reynolds equations. It is found that the improvements of these slip models and the corresponding slip-corrected Reynolds equations are of limited use in the air bearing simulation of molecular gas lubrication. The problem of a contact pressure singularity inherent in the FK model needs to be further analyzed.

Nomenclature

a = surface accommodation factor ($a = \frac{2-\alpha}{\alpha}$)

D = inverse Knudsen number

h = spacing between the slider and disk or air bearing film thickness

h_0 = characteristic spacing between the slider and the disk

H = non-dimensional form of h ($H=h/h_0$)

k = Boltzmann constant

Kn = Knudsen number ($Kn=\lambda/h$)

L = characteristic length or the radius of the base of an asperity

m = mass of a molecule

N = molecular number density

n = unit outer normal of a boundary

p = air bearing pressure

p_a = ambient air pressure

P = non-dimensional air bearing pressure ($P=p/p_a$)

$Q_{P,con}$ = non-dimensional flow rate or flow rate coefficient for continuum Poiseuille flow

$$(Q_{P,con} = D/6)$$

Q_P = non-dimensional flow rate or flow rate coefficient for Poiseuille flow

$Q_{C,con}$ = non-dimensional flow rate or flow rate coefficient for continuum Couette flow

$$(Q_{C,con} = 1)$$

Q_C = non-dimensional flow rate or flow rate coefficient for Couette flow

\bar{Q}_P = relative Poiseuille flow rate coefficient ($\bar{Q}_P = Q_P / Q_{P,con}$)

\bar{Q}_C = relative Couette flow rate coefficient ($\bar{Q}_C = Q_C / Q_{C,con}$)

R = gas constant for 1 g gas (R = universal gas constant / gas molecular weight)

T = gas temperature

u = gas flow velocity

U = velocity of the bearing surface or the disk

u_{slip} = slip velocity of the rarefied gas on a stationary wall

U_{slip} = non-dimensional form of u_{slip} ($U_{slip} = u_{slip}/U$)

\bar{v} = average molecular speed ($\bar{v} = \frac{2}{\sqrt{\pi}} \sqrt{2RT}$)

α = surface (momentum) accommodation coefficient

λ = mean free path of gas molecules

λ_a = mean free path of gas molecules at the ambient pressure

λ_m = modified mean free path

μ = viscosity

τ = shear stress

ρ = gas density ($\rho = mN$)

2. *Slip models and slip corrected Reynolds equations*

Slip models are the bases of slip-corrected compressible Reynolds equations. A compressible Reynolds equation is derived from the Navier-Stokes equations with velocity boundary conditions, the conservation of the mass flow rates, the equation of state of the compressible flow and the velocity boundary condition. In hard disk drives the disk's rotation velocity is low subsonic. Usually it is assumed that the flow is isothermal, the pressure field is uniform in the film thickness direction, the inertial effects are negligible and the viscosity change due to the position and velocity is also negligible. The slip model prescribes the velocity boundary condition due to rarefaction, which usually depends on the velocity profile near the wall, the Knudsen number, the surface accommodation coefficient, the flow velocity gradient or pressure gradient or shear stress at the wall.

In general the obtained slip-corrected Reynolds equations have the form,

$$\nabla \cdot [(\bar{Q}_p ph^3 \nabla p) - 6U \mu ph] = 12\mu \frac{\partial(ph)}{\partial t}, \quad (1)$$

where \bar{Q}_p is the relative Poiseuille flow rate coefficient. The deviation of its value from 1 represents the effect of the velocity slip on the gas flow. Its expression in terms of the (inverse) Knudsen number depends on the slip model used in the derivation.

Usually a compressible slip-corrected Reynolds equation does not contain the relative Couette flow rate coefficient, provided that the surface accommodation coefficients on both boundaries are close to each other. The surface accommodation coefficient is defined for the tangential momentum exchange of gas molecules with surfaces and it determines the velocity slip property of the boundary for slip flows. Due to the skew symmetry of Couette flow with respect to its center plane, the Couette flow rate does not depend on the velocity slip at the boundaries, provided that the slip conditions at the upper and lower boundaries are the same. On the contrary, the symmetry of Poiseuille flow with respect to the center plane results in a strong dependence of the Poiseuille flow rate on the slip conditions at the boundaries.

2.1 Classical first-order [5], second-order [6] and 1.5-order [7] models

Usually the temperatures of the slider and the disk surfaces are close to the ambient temperature. The air bearing film can be assumed to be isothermal, which has been validated using the linearized Boltzmann equation with the BGK model [1], and the thermal creep effect can be neglected in the velocity slip at the boundaries. Hence the first-order slip model, which was originally proposed by Maxwell in 1879 and contains the velocity jump and thermal creep, can be reduced to [3],

$$u_{slip} = \frac{2-\alpha}{\alpha} \lambda \frac{du}{dn}. \quad (2)$$

Burgdorfer [5] used this velocity slip model from Schaaf and Sherman's work on slip flow [4] and derived a first-order slip-corrected Reynolds equation. A second-order slip model,

$$u_{slip} = \frac{2-\alpha}{\alpha} \left(\lambda \frac{du}{dn} - \frac{\lambda^2}{2} \frac{d^2u}{dn^2} \right), \quad (3)$$

was derived by Hsia and Domoto [6] and a new slip-corrected Reynolds equation was obtained. Hsia and Domoto also compared this Reynolds equation to their experimental results. This slip model has more of a mathematical basis than a physical basis.

Equating the kinetic-theory based momentum transfer rate on a stationary wall and the macroscopic shear stress, Mitsuya [7] derived a “1.5-order” slip model,

$$u_{slip} = \frac{2-\alpha}{\alpha} \lambda \frac{du}{dn} - \frac{1}{2} \left(\frac{2\lambda}{3} \right)^2 \frac{d^2u}{dn^2}. \quad (4)$$

Although it is referred to as a 1.5-order slip model, it is actually a second-order type model, since the slip velocity contains the second order effect of the mean free path (or Kn in a non-dimensional sense).

2.2 Wu’s pressure gradient model [8] and new first- and second-order models [9]

Equating the macroscopic shear stress at the wall and the shear stress obtained from kinetic theory, Wu and Bogy proposed a pressure gradient model [8] and new first- and second-order slip models [9]. In the first model, the macroscopic shear stress is obtained from the balance of forces on a control volume with its height equal to the mean free path, which is shown in Figure 1(a), and it is expressed in the form,

$$\tau|_{z=0} = \mu \frac{\partial u}{\partial z} \Big|_{z=0} - \lambda \frac{\partial P}{\partial x} \Big|_{z=0}, \quad (5)$$

which is different from the conventional formula $\tau = \mu \frac{\partial u}{\partial z}$ of fluid mechanics for slip and continuum flows.

The kinetic theory based shear stress is the momentum transfer rate from the gas

molecules to the solid wall [3], which is expressed as

$$\tau = \frac{\rho \bar{v} \alpha u_{slip}}{2(2 - \alpha)} \quad (6)$$

The slip velocity, obtained by equating these two expressions, is then,

$$u_{slip} = \frac{2 - \alpha}{\alpha} \left(\lambda \frac{\partial u}{\partial z} - \frac{2\lambda}{\rho \bar{c}} \frac{\partial P}{\partial x} \right). \quad (7)$$

The existence of the pressure gradient in the model is consistent with the fact that it is essentially a second-order slip type model. Using one of the reduced Navier-Stokes equations of Wu [8],

$$0 = -\frac{\partial p}{\partial x} + \mu \frac{\partial^2 u}{\partial y^2}, \quad (8)$$

and the viscosity of the hard sphere model $\mu = \frac{1}{2} m N \bar{v} \lambda$ [3], the slip model in Equation (7) changes to a second-order form,

$$u_{slip} = \frac{2 - \alpha}{\alpha} \left(\lambda \frac{\partial u}{\partial z} - \lambda^2 \frac{\partial^2 u}{\partial z^2} \right). \quad (9)$$

In the derivation of the new first- and second-order slip models [9], the conventional formula $\tau = \mu \frac{\partial u}{\partial z}$ is used for the macroscopic shear stress at the boundary. The kinetic analysis of the momentum transfer rate, which still uses integration based on the continuum media assumption, obtains an expression of viscosity,

$$\mu = \frac{1}{3} m N \bar{v} \lambda. \quad (10)$$

This equation is slightly different from the conventionally used expression of viscosity for the hard elastic sphere gas molecule model [19],

$$\mu \approx \sqrt{\frac{2RT}{\pi}} \rho \lambda = \frac{1}{2} m N \bar{v} \lambda, \quad (11)$$

which is also used in the derivation of the pressure gradient model [8].

2.3 Shen and Chen's model [13]

Shen and Chen [13] did not solve the Boltzmann equation for the air bearing film, although the derivation of their slip model started from the linearized Boltzmann equation. With the linearized Boltzmann equation and a restriction of the flow to Poiseuille type with $u=u(y)$ and $P=P(x)$, shown in Figure 1(b), Shen and Chen [13] obtained the shear stress in the flow in the form of,

$$\tau = n \tau k T \frac{du}{dy} = \mu \frac{du}{dy}, \quad (12)$$

and the shear stress at the wall in the form of,

$$\tau|_{y=0} = \alpha \left[\sqrt{\frac{kT}{2\pi m}} u|_{y=0} mn + \frac{1}{2} n k T \frac{du}{dy} \Big|_{y=0} \right], \quad (13)$$

For the hard sphere ideal gas molecule model, we have $P = \rho RT$ and $\mu = n \tau k T$. Hence the above Equation (13) can be rewritten as,

$$\tau|_{y=0} = \alpha \left[\frac{\mu}{2\lambda} u|_{y=0} mn + \frac{\mu}{2} \frac{du}{dy} \Big|_{y=0} \right]. \quad (14)$$

Instead of equating the internal shear stress at the flow boundary, shown by Equation (12) evaluated at the wall ($y=0$), and the shear stress at the wall, i.e. Equation (13), and then producing the classical first-order slip model, Shen and Chen [13] adopted the balance equation of forces on a control volume at the wall. The control volume has a height equal

to the so-called effective mean free path. The force balance equation produces an expression for the slip velocity,

$$u_{slip} = u|_{y=0} = \frac{2-\alpha}{\alpha} \left(\frac{\pi kT}{2m} \right)^2 \frac{du}{dy} \Big|_{y=0} - \frac{\lambda_m}{\alpha} \sqrt{\frac{2\pi m}{kT}} \frac{1}{mn} \frac{dp}{dx}. \quad (15)$$

Using the hard sphere gas molecule model, this can be changed to

$$u_{slip} = u|_{y=0} = \frac{2-\alpha}{\alpha} \left(\lambda_m \frac{du}{dy} \Big|_{y=0} - \frac{2}{2-\alpha} \frac{\lambda_m^2}{\mu} \frac{dp}{dx} \right). \quad (16)$$

As in the derivation of the pressure gradient model [8], the force balance equation does not produce the final slip velocity expression in Equation (16) until the approximation

$\frac{du}{dy} \Big|_{y=\lambda_m} \text{ (or } \lambda) \approx \frac{du}{dy} \Big|_{y=0}$ is used, which is not based on any kinetic theories. It is seen that

this approximation is not valid for a transition flow, which has $0.1 < Kn < 10$. The mean free path is comparable to the thickness of the gas film, so it can not be approximated as zero.

It is interesting to note that this slip model is very similar to Wu's pressure gradient model [8], except for the mean free path and the factor $\frac{2}{2-\alpha}$ in the second term. With Equation (15) and the conservation of linear moment for the Poiseuille flow, the slip velocity can be finally expressed as,

$$u_{slip} = u|_{y=0} = \frac{2-\alpha}{\alpha} \left(\lambda_m \frac{du}{dy} \Big|_{y=0} - \frac{2}{2-\alpha} \lambda_m^2 \frac{d^2u}{dy^2} \right) \quad (17)$$

Essentially this is still a second-order slip type model, since its non-dimensional expression contains the square of the Knudsen number.

2.4 Bahukudumbi and Beskok's slip model [15]

Using a modified slip boundary condition for steady plane Couette flow [16],

$$u_{slip} = \frac{2-\alpha}{\alpha} (1.2977 + 0.71851 \tan^{-1}(-1.17488Kn^{0.58642})) \lambda \frac{du}{dy}, \quad (18)$$

and a generalized high-order slip boundary condition for the pressure-driven flow [17],

$$u_{slip} = \frac{2-\alpha}{\alpha} \left(\frac{Kn}{1+Kn} \right) \lambda \frac{du}{dy}. \quad (19)$$

Bahukudumbi and Beskok [15] derived a phenomenological Reynolds equation valid for a wide range of Knudsen numbers. An interesting point is that Equation (19) is only valid for the non-dimensional velocity profile of Poiseuille flow. The Poiseuille flow rate coefficient based on Equation (19) differs greatly from the DSMC results [17]. With a modification of dynamic viscosity, a modified Poiseuille flow rate coefficient is proposed [15 and 17],

$$Q_p = (1 + \delta Kn) \left(1 + \frac{6Kn}{1+Kn} \right), \quad (20)$$

where the rarefaction correction parameter δ (denoted by α in [15 and 17]) is obtained by matching the modified flow rate coefficient with the Poiseuille flow rate database via the solution of a two-dimensional linearized Boltzmann equation [20]. So it is not surprising that their analytical lubrication equation gives similar results to those of the FK lubrication equation with its numerically obtained look-up table [20]. A good point is that their model also gives the analytical expressions for the flow velocity profile and shear stress at the boundaries with good accuracy for flows with $Kn < 12$. This is an advantage over the FK lubrication equation, however, no improvement to the air bearing simulation.

2.5 Other kinetic-theory based slip models

Although not integrated into the Reynolds lubrication equation, a series of second-order slip models have been proposed for shear or pressure driven flows, such as the models by Schamberg [21], Beskok and Karniadakis [17], Cercignani and Daneri [22], Deissler [23], Hadjiconstantinou [24]. Beskok and Karniadakis [17] also derived higher-order slip models.

The slip velocity of all of the second-order slip models can be expressed in a general form, when the surface accommodation coefficient is 1,

$$U_{slip} = C_1 Kn \left(\frac{\partial U}{\partial n} \right) \Big|_{boundary} - C_2 Kn^2 \left(\frac{\partial^2 U}{\partial n^2} \right) \Big|_{boundary} \quad (21)$$

These models are only valid in the slip flow regime and not for the entire Knudsen number regime. Table 1 lists the coefficients C_1 and C_2 for all of the second-order slip models referred to in this report. In this table the first- and 1.5- order slip models are viewed as second-order slip models with special coefficients C_1 and C_2 .

Corresponding to the general slip model in Equation (21), the Poiseuille flow rate coefficient is,

$$Q_p = \frac{D}{6} + C_1 \frac{\sqrt{\pi}}{2} + C_2 \frac{\pi}{2D}. \quad (22)$$

Figure 2 shows plots of the Poiseuille flow rate of the FK model, the first-, 1.5- and second-order slip models, the pressure gradient model [8] and Shen and Chen's model [13]. It is seen that in the transition flow and free molecular flow regions ($D < 8.86$) the slip models, which can be expressed by Equation (21), differ greatly from the FK model in predicting the Poiseuille flow rate. This is expected since the slip model is only valid

in the slip flow region.

2.6 Mathematical-interpolation based slip models

Based on an analogy to high-order slip models, Hwang's modified Reynolds equation [10] assumes the slip velocity in the form of,

$$u_{slip} = A\lambda \frac{\partial u}{\partial y} - \frac{1}{2} BD^C h^2 \frac{\partial^2 u}{\partial y^2} \quad (23)$$

The corresponding Poiseuille flow rate coefficient is expressed as,

$$Q_p = \frac{D}{6} + A \frac{\sqrt{\pi}}{2} + BD^{1+C}. \quad (24)$$

Parameters A , B and C are obtained by mathematically fitting the flow rate coefficient expression to the result of the linearized Boltzmann equation.

Taking almost the same approach, Ng's multi-coefficient slip-corrected Reynolds equation [11] has the slip velocity in the form,

$$u_s = A\lambda \frac{\partial u}{\partial y} - BK n^C \lambda^2 \frac{\partial^2 u}{\partial y^2}. \quad (25)$$

The corresponding Poiseuille flow rate coefficient is,

$$Q_p = \frac{D}{6} + A \frac{\sqrt{\pi}}{2} + 2B \left(\frac{\pi}{4}\right)^C D^{-(1+C)}. \quad (26)$$

However Equation (26) is incorrect. This can be seen if we take the Hsia and Domoto's second order slip model as an example. Their second-order slip model has $A = 1$, $B = 1/2$

and $C = 0$ while its $Q_p = \frac{D}{6} + \frac{\sqrt{\pi}}{2} + \frac{\pi}{4D}$ does not agree with Equation (26). Ng's

parameters, A , B and C , are obtained by fitting Equation (26) to the numerical results of

the Boltzmann equation using a mathematics- based engineering quality control method.

Ng's stress-density ratio slip-corrected Reynolds equation [12] took a similar approach. To accommodate Maxwell's first order slip model, the slip velocity is forced to take a form of,

$$u_s = C_s \frac{\tau}{\rho}, \quad (27)$$

where the parameter C_s is called the slip coefficient and for the Maxwell 1-order slip model,

$$C_s = \left(\frac{2}{\alpha} - 1\right) \frac{1}{\sqrt{2RT/\pi}}. \quad (28)$$

The parameter C_s is calculated through fitting Equation (27) to the shear stress and slip velocity obtained using the DSMC method. With $\alpha = 1$, $p_a = 1$ atm and $T = 273$ K, the slip coefficient C_s , suitable especially to the transition flow regime, is calculated to universally be 0.047 s/m. Notice that Equation (28) obtains $C_s = 0.026$ s/m for the first-order slip flow, which is valid in the slip flow regime. The slip model shown by Equation (27) is not consistent in the regime between the slip flows and the transition flows, where Kn is around 0.1. This inconsistency makes this stress-density slip model [12] questionable.

Obviously, these mathematically obtained slip models and slip-corrected Reynolds equations lack any physical basis.

3. Modification of the mean free path

The mean free path of gas molecules is the mean value of the free distances that gas

molecules can travel between two collisions in the equilibrium state. It depends on the molecule's internal structure, gas pressure and temperature. Based on kinetic theory, different air molecule models give different expressions for the mean free path.

3.1 Probabilistic mean

It is obvious that the free distance that a gas molecule in an air bearing film can travel before a collision with another molecule or the boundary is reduced due to the existence of the boundaries. The second-order slip models [6, 8 and 13] either take the Taylor expansion of the bulk velocity with respect to the mean free path or employ a control volume with a height related to the mean free path. So it may be more accurate if the mean free path in the second-order slip models is replaced by a modified mean free path in considering the existence of boundaries. Peng et. al. [14] obtained the probabilistic mean of the mean free path considering the boundary effects,

$$\lambda_m = \begin{cases} \lambda(1 - \frac{\lambda}{4h}), & h \geq \lambda \\ \lambda(\frac{3h}{4\lambda} - \frac{h}{2\lambda} \ln(\frac{h}{\lambda})), & h < \lambda \end{cases} \quad (29)$$

Three assumptions are adopted in the derivation process. For the air flow, it is assumed that the air molecules are uniformly distributed in the air film and the velocity directions of air molecules are uniformly distributed in the 3-dimensional space. In their derivation it is also assumed that collision with another molecule is almost sure to happen when one molecule travels a distance of its mean free path. This inherent assumption can be seen from their result that the mean free path of molecules with a distance $d > \lambda$ from

the boundary is not changed due to the boundary effects. Specifically, Figure 3 shows it is not possible for the molecule to travel more than λ in the direction to the boundary before collision, while the possibility is finite if there is no boundary. This boundary effect is neglected under that inherent assumption.

With the mean free path modification, an agreement between high order slip-corrected Reynolds equations and the FK model is obtained. The mean free path in the slip models can be replaced by the modified mean free path in Equation (29), resulting in a more reasonable choice of the Taylor expansion variable and the control volume's height. With this replacement, the 1.5- or second-order slip-corrected Reynolds equations predict a pressure distribution and a load capacity close to those of the FK model, although the first-order slip-corrected Reynolds equation does not change much; and the Poiseuille flow rates of the 1.5- and second-order slip model have a similar trend to that of the FK model in the entire Knudsen number regime.

However, it appears that the approach of modifying the mean free path cannot replace the FK model. It is obvious that the three assumptions used in Peng's derivation are not valid for a real air bearing flow. The distribution of molecular velocities is described by the Boltzmann equation. For an ideal gas, the number density of the air molecules, related to the density, is proportional to the gas pressure which is not necessarily uniform. The third assumption neglects the randomness of molecular collisions. Thus, it is supposed to be better if the true mean free path considering the boundary effects can be calculated directly from the velocity distribution function of gas molecules in the Boltzmann

equation for the air bearing film. On the other hand, after the solution of the Boltzmann equation for the air bearing film is obtained, the air bearing problem is solved and the air pressure, the macroscopic flow velocity, the shear stress and so on can be obtained in terms of integrals with the molecular velocity distribution. The slip-corrected Reynolds equation becomes unnecessary. In this sense, one should not expect to replace the FK model with a slip-corrected Reynolds equation that uses a modified mean free path.

The mean free path modification is not necessary for the FK model. In that model the mean free path is a characteristic value of the BGK gas molecules in the equilibrium state. The boundary effect is considered by the boundary conditions for the linearized Boltzmann equation. So Peng's further implementation of the modified mean free path into the FK model is not necessary.

3.2 The Matthiessen rule

The effective mean free path in Shen and Chen's slip model [13] is calculated using the Matthiessen rule [25],

$$\frac{1}{\lambda_m} = \frac{1}{\lambda / \sqrt{3}} + \frac{1}{h/2}. \quad (30)$$

The Matthiessen rule is widely used in considering the boundary scattering effects for electron and phonon transport. However, it is seldom used for rarefied gas dynamics. This effective mean free path can not be taken as a modified mean path of air molecules. A discrepancy occurs when the air film thickness h becomes much larger than the mean free path. As h increases, the boundaries move away from most of the air molecules, the

boundary effect diminishes and the mean free path should approach the original mean free path λ instead of $\lambda/\sqrt{3}$. Without this effective mean free path, Shen and Chen's slip model is a second-order type, and the corresponding Poiseuille flow rate is no longer close to that predicted by the FK model.

3.3 Air molecule models

The hard sphere model is usually used to calculate the mean free path used in the slip models. Sun et. al. [18] took the results of a variable hard sphere (VHS) model [26] and variable soft sphere (VSS) model [27] and applied the modified mean free path to the classical second-order slip model. However, they compared their results to those of the slip-corrected Reynolds equations and the linearized Boltzmann equation with the BGK model. So this comparison may not validate the application of VHS and VSS models to an air bearing lubrication.

4. Contact pressure singularity

It was stated in Wu and Bogy [8] that their second-order slip-corrected Reynolds equation does not predict an unphysical unbounded pressure singularity in the limit of contact between the bearing surface and the moving surface. Following Wu's analysis [8], we can change the form of the Reynolds equation (1), by using the second-order slip flow's Poiseuille flow rate coefficient in Equation (22), to the following form for the steady state 1-dimensional air bearing,

$$\frac{\partial}{\partial X} \left[\left(\frac{p_a h_0^2}{6\mu UL} PH^3 + \frac{\beta p_a \lambda_a h_0}{6\mu UL} H^2 + \frac{\gamma p_a \lambda_a^2 H}{6\mu UL P} \right) \frac{\partial P}{\partial X} \right] = \frac{\partial}{\partial X} (PH), \quad (31)$$

where $\beta=6a$ and $\gamma=6a$ (12a) for Hsia and Domoto's second-order slip model [6] (Wu's pressure gradient model [8]). In the near-contact regime, H approaches zero. Neglecting the high order terms of H in Equation (25), the Reynolds equation can be reduced to,

$$\frac{\partial}{\partial X} \left[\Gamma \frac{H}{P} \frac{\partial P}{\partial X} \right] = \frac{\partial}{\partial X} (PH), \quad (32)$$

where the dimensionless parameter $\Gamma = \frac{\gamma p_a \lambda_a^2}{6\mu UL}$. Wu's asymptotic solution of Equation

(31) for an asperity with actual contact at $X = 0$, the profile of which is $H = \frac{AL^2}{h_0} X^2 + 1$

and shown in Figure 4, is

$$P = \begin{cases} \frac{P_L \Gamma}{\Gamma - P_L(1+X)}, & -1 \leq X < 0 \\ \frac{P_R \Gamma}{\Gamma + P_R(1-X)}, & 0 < X \leq 1 \end{cases}, \quad (33)$$

where P_L and P_R are the non-dimensional air bearing pressures at the left and right side of the contact regime. As shown by Wu, this solution has a shock wave like discontinuity at the contact point. However, a special situation is not discussed by Wu. Provided that the same boundary condition is taken with $P_L = P_R = 1$, Equation (33) may produce an unbounded air pressure before the contact point $X = 0$ if $\Gamma = 1$. The parameter values used by Wu [8] for an asperity in near contact with the disk are $p_a = 0.101$ mPa, $\lambda_a = 65$ nm, $U = 10$ m/s, $\mu = 1.85 \times 10^{-5}$ N·s/m² and $L = 0.5 \mu\text{m}$. It is obvious that if the accommodation coefficient is 1 and $L = 2.284 \mu\text{m}$ for $\gamma = 6$ ($L = 4.568 \mu\text{m}$ for $\gamma = 12$), which are still reasonable parameter values for the characteristic length of an asperity, unbounded pressure values can be obtained near the contact point. So it is possible that a

second-order slip-corrected Reynolds equation also predicts an unphysical unbounded pressure singularity in the limit of contact with a certain asperity profile, which contradicts Wu's conclusion.

Numerical simulations are carried out here to compare with this asymptotic analysis. A slider with a length of 0.04 mm and a width of 0.04 mm has an asperity at the center of the flat air bearing surface. The asperity has a parabolic shape of $H = \frac{AL^2}{h_0} r^2 + 1$, where r is the distance from the center. The slider has fixed zero pitch and roll angles on a disk with 10000 RPM. The CML air bearing program is used to calculate the air bearing pressure profile. The FK model, the pressure gradient model [8] and the classical second-order slip model [6] are used in the air bearing simulation, respectively. Three cases with different parameter values are analyzed – Case 1 with $A = 10^4$ /m and $L = 0.5$ μm ; Case 2 with $A = 10^2$ /m and $L = 5$ μm and Case 3 with $A = 25$ /m and $L = 10$ μm . These micron level values are reasonable for L , the radius of the base of a parabolic asperity. A is the shape parameter of the parabolic profile and here a value of A is chosen so that the asperity tip has a height of 2.5 nm above its base in each case, which is a reasonable height value.

Simulation results of Case 1 are shown in Figure 5, including the ABS profile and air bearing pressure profile along the center line for a minimum flying height (min FH, i.e. the gap between the asperity tip and the disk) of 0.1 nm, 0.01 nm and 0.001 nm. They are similar to Wu's simulation results. The air bearing pressure along the center line obtained

using the pressure gradient model has a shock wave like shape across the near-contact regime, while the air bearing pressure obtained using the FK model has a very large value in the near-contact regime. As the min FH decreases from 0.1 nm to 0.001 nm, the pressure profile obtained using the pressure gradient model converges to a bounded value, while the pressure profile obtained using the FK model has an increasing air pressure in the near-contact regime. These conclusions with Case 1 agree well with Wu's conclusions.

The ABS profiles and air bearing pressures along the slider's center line of Cases 2 and 3 are plotted in Figures 6 and 7, respectively. It is obvious in both of these cases that the air bearing pressures obtained using either the FK model or the pressure gradient model do not converge to a bounded value. The air bearing pressure at the near-contact regime increases beyond 100 atm or even 1000 atm, as the min FH decreases. Further, the results of the classical second-order slip-corrected Reynolds equation for Cases 1, 2 and 3 are shown in Figure 8. The rapid increase of the air bearing pressure at the near-contact region as the gap decreasing does not change for Cases 2 and 3. A shock wave like profile of the air bearing pressure at the near-contact region is not a universal result of a second-order type slip-corrected Reynolds equation.

As a conclusion, neither the pressure gradient model nor the classical second-order slip model always predicts a bounded air bearing pressure at the contact or near-contact region. This contact pressure singularity may be associated with the usage of the ideal gas law $p=\rho RT$. As the film thickness approaches zero at the near-contact region, the gas

density there approaches infinity. As a result, the pressure also approaches infinity at the near-contact region. Therefore, the contact singularity of the Reynolds lubrication theory needs further analysis.

5. *Conclusions*

A valid slip model for Poiseuille flow is critical to obtaining a slip-corrected Reynolds equation, when the surface accommodation coefficients at the slider surface and bearing surface are the same or close to each other. Different slip models predict different slip conditions at the slider and the disk surfaces, and then lead to different Poiseuille flow rate coefficients, i.e. the non-dimensional Poiseuille flow rates, which are the only varying part in the different slip-corrected Reynolds equations.

Through modifying the mean free path or mathematically matching the Poiseuille flow rate to the kinetic simulation results, some slip-corrected Reynolds equations can give close results to that of the FK model based on the linearized Boltzmann equation [1]. However, it is not expected that these can replace the FK model and give more acute results. The contact pressure singularity is a common problem of the second-order type slip-corrected Reynolds equation as well as the FK lubrication equation. It may be related to the application of the ideal gas law, and it needs further consideration.

Reference

- [1] S. Fukui and R. Kaneko, "Analysis of ultra-thin gas film lubrication based on linearized Boltzmann equation: First report-derivation of a generalized lubrication equation including thermal creep flow," *ASME Journal of Tribology*, vol. 110, pp. 253-262, 1988
- [2] P. L. Bhatnagar, E. P. Gross and M. Krook, "A model for collision processes in gases. I. Small amplitude processes in charged and neutral one-component systems," *Physics Review*, vol. 94, no. 3, pp. 511-525, 1954.
- [3] E. H. Kennard, *Kinetic Theory of Gasses*, MacGraw-Hill Book Co. Inc., New York, 1938.
- [4] S. A. Schaaf and F. S. Sherman, "Skin friction in slip flow," *Journal of Aeronautical Sciences*, vol. 21, no. 2, pp. 85-90, 1953.
- [5] A. Burgdorfer, "The influence of the molecular mean free path on the performance of hydrodynamic gas lubricated bearings," *ASME Journal of basic Engineering*, vol. 81, no.1, pp. 94-100, 1959.
- [6] Y. T. Hsia and G. A. Domoto, "An experimental investigation of molecular rarefaction effects in gas lubricated bearings at ultra-low clearance," *ASEM Journal of Tribology*, vol. 105, pp. 120-130, 1983.
- [7] Y. Mitsuya, "Modified Reynolds equation for ultra-thin film gas lubrication using 1.5-order slip-flow model and considering surface accommodation coefficient," *ASME Journal of Tribology*, no. 2, pp.289-294, 1993.

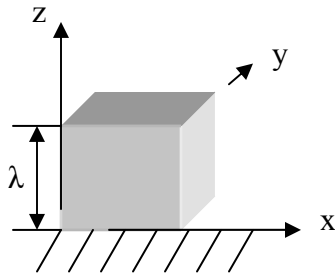
- [8] L. Wu and D. B. Bogy, "A generalized compressible Reynolds lubrication equation with bounded contact pressure," *Physics of Fluids*, vol. 13, no. 8, pp. 2237-2244, 2001.
- [9] L. Wu and D. B. Bogy, "New first and second order slip models for the compressible Reynolds Equation," *ASME Journal of Tribology*, vol. 125, pp. 558-561, 2003.
- [10] C. C. Hwang, R. F. Fung, R. F. Yang, C. I. Weng and W. L. Li, "A New Modified Reynolds Equation for Ultrathin Film Gas Lubrication," *IEEE Transaction on Magnetics*, vol. 32, no. 2, 1996.
- [11] E. Y.-K. Ng, N. Liu and X. Mao, "Stress-density ratio slip-corrected Reynolds equation for ultra-thin film gas bearing lubrication," *Physics of Fluids*, vol. 14, no. 4, pp. 1450-1457, 2002.
- [12] E. Y.-K. Ng and N. Liu, "A Multicoefficient Slip-Corrected Reynolds Equation for Micro-Thin Film Gas Lubrication", *International Journal of Rotating Machinery*, vol. 2005, pp 105-111, 2005.
- [13] S. Shen and G. Chen, "A kinetic-theory based first order slip boundary condition for gas flow," *Physics of Fluids*, vol. 19, pp. 086101, 2007.
- [14] Y. Peng, X. Lu and J. Luo, "Nanoscale Effect on Ultrathin Gas Film Lubrication in Hard Disk Drives," *ASME Journal of Tribology*, vol. 126, pp. 347-352, 2004.
- [15] P. Bahukudumbi and A. Beskok, "A phenomenological lubrication model for the entire Knudsen regime," *Journal of Micromechanics and Microengineering*, vol. 13, no. 6, pp. 873-884, 2003.

- [16]P. Bahukudumbi, J. H. Park and A. Beskok, "A unified engineering model for steady and quasi-steady shear driven gas micro flows," *Microscale thermophysical Engineering*, vol. 7, no. 4, pp. 291-315, 2003.
- [17]A. Beskok and G. E. Karniadakis, "A model for flows in channels, pipes and ducts at micro and nano scales," *Microscale thermophysical Engineering*, vol. 3, no. 1, pp. 43-77, 1999.
- [18]Y. Sun, W. K. Chan and N. Liu, "A slip model with molecular dynamics," *Journal of Micromechanics and Microengineering*, vol. 12, pp. 316-322, 2002.
- [19]S. Chapman and T. G. Cowling, *The Mathematical Theory of Non-Uniform Gases*, 3rd ed, Cambridge University Press, New York, NY.
- [20]S. Fukui and R. Kaneko, "A database for interpolation of Poiseuille flow rates from high Knudsen number lubrication problems," *ASME Journal of Tribology*, vol. 112, pp. 78-83, 1990.
- [21]R. Schamberg, *The fundamental Differential Equations and the boundary conditions for High Speed slip-Flow, and their application to several specific Problems*, Ph.D. thesis, California Institute of Technology, 1947.
- [22]C. Cercignani and A. Daneri, "Flow of a rarefied gas between two parallel plates," *Journal of Applied Physics*, vol. 43, pp. 3509-3513, 1963.
- [23]R. G. Deissler, "An analysis of second-order slip flow and temperature jump boundary conditions for rarefied gases," *International Journal of Heat Mass Transfer*, vol. 7, pp. 681-694, 1964.

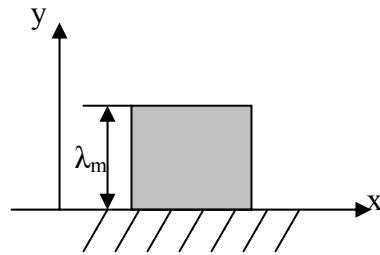
- [24]N. G. Hadjiconstantinou, “Comment on Cercignani’s second-order slip coefficient,” *Physics of Fluids*, vol. 15(8), pp. 2352-2354, 2003.
- [25]N. W. Ascroft and N. D. Mermin, *Solid State Physics*, Saunders College, Philadelphia, 1976.
- [26]G. A. Bird, *Molecular Gas Dynamics and the Direct Simulation of Gas Flows*, Oxford: Clarendon, 1994.
- [27]K. Koura and H. Matsumoto, “Variable soft sphere molecular model for inverse -power-law or Lennard-Jones potential,” *Physics of Fluids*, vol. 4, pp. 1083-1085, 1992.

Table 1 Coefficients for second-order slip models expressed in a general form

Model developers	C_1	C_2
Maxwell [3] (1938)	1	0
Schamberg [21] (1947)	1	$5\pi/12$
Cercignani and Daneri [22] (1963)	1.1466	0.9756
Deissler [23] (1964)	1	$9/8$
Hsia and Domoto [6] (1983)	1	0.5
Mitsuya [7] (1993)	1	$2/9$
Beskok and Karniadakis [17] (1999)	1	-0.5
Wu and Bogy [8] (2001)	1	1
Wu and Bogy [9] (2003)	$2/3$	$1/4$
Hadjiconstantinou [24] (2003)	1.1466	0.647
Shen and Chen [13] (2007)	1	2



(a) Control volume used by Wu and Bogy [8]



(b) Control volume used by Shen and Chen [13]

Fig. 1 Control volume with different heights used to derive the force balance equation.

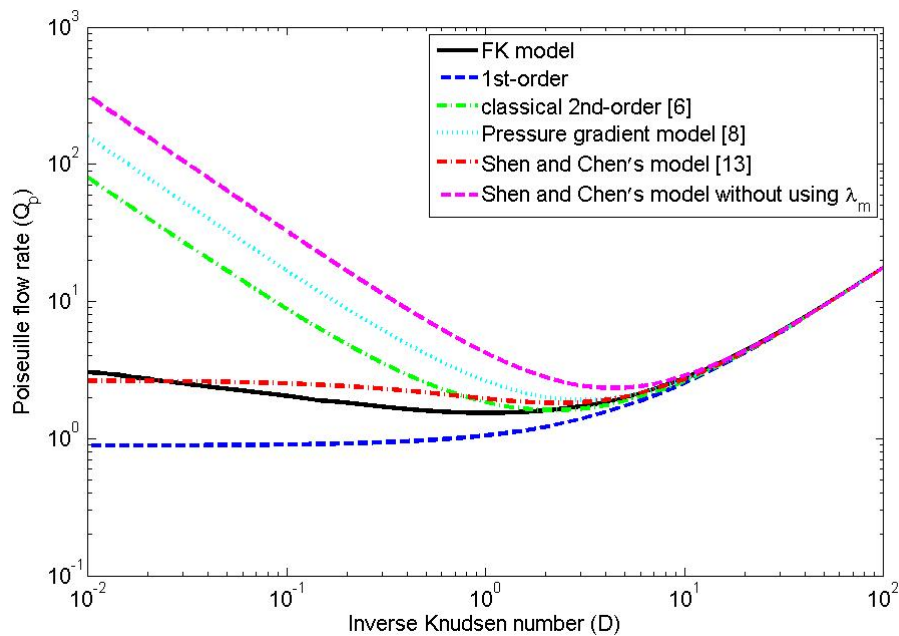


Fig. 2 The relation between the Poiseuille flow rate coefficient (non-dimensional Poiseuille flow rate) and the inverse Knudsen number in the FK model, the first- and second-order models, the pressure gradient model [8] and Shen and Chen's model [13].

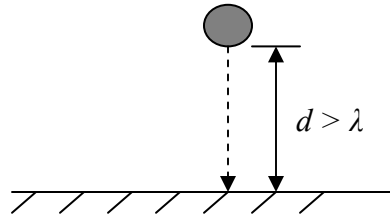


Fig. 3 One molecule and one boundary.

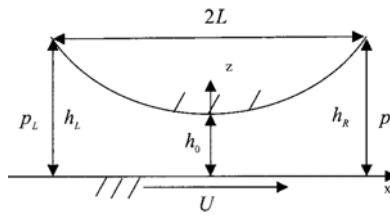
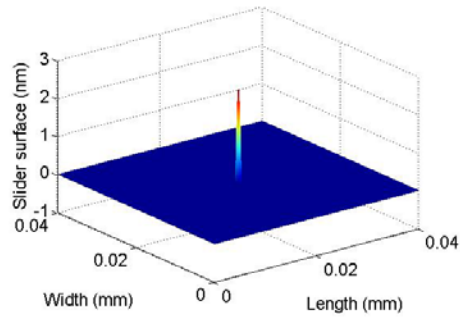
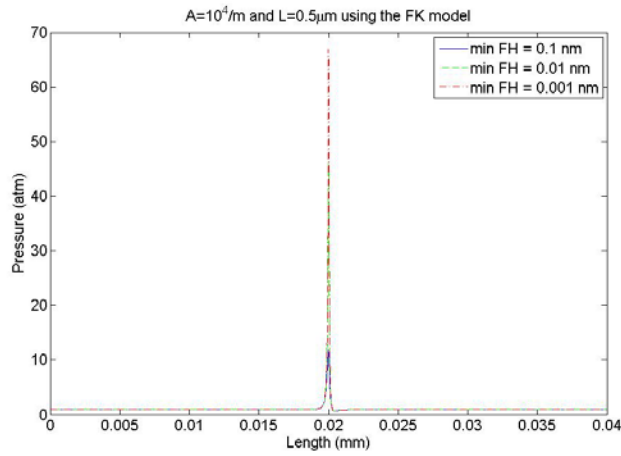


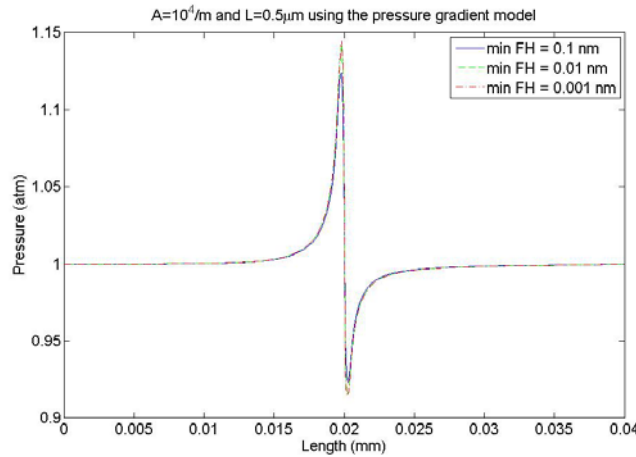
Fig. 4 Parabolic profile of an asperity in near-contact with the disk [8].



(a) Air bearing surface profile

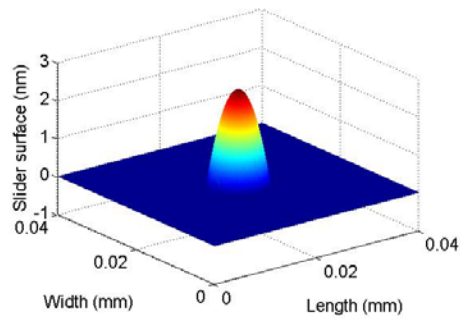


(b) Air bearing pressure profile along the ABS's center line using the FK model

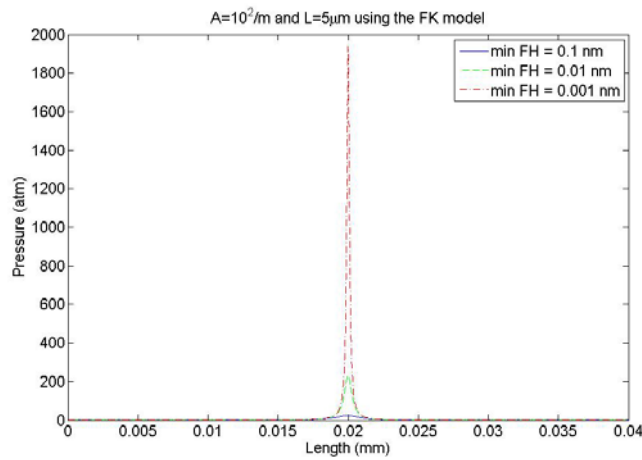


(c) Air bearing pressure profile along the ABS's center line using the pressure gradient model

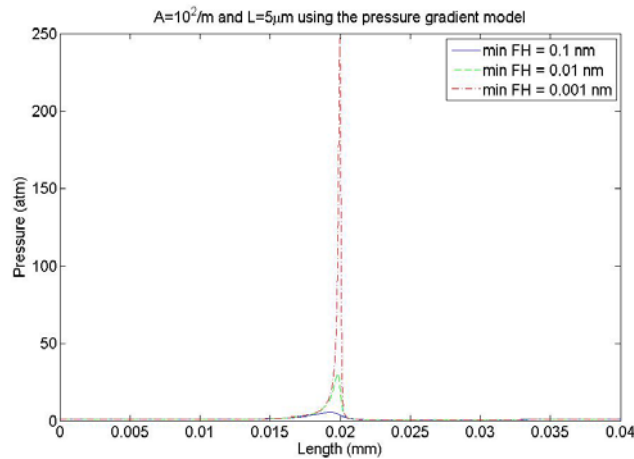
Fig. 5 ABS profile and air bearing pressure profile along the center line from the leading edge to the trailing edge in Case 1 ($A = 10^4 / \text{m}$ and $L = 0.5 \mu\text{m}$).



(a) Air bearing surface profile.

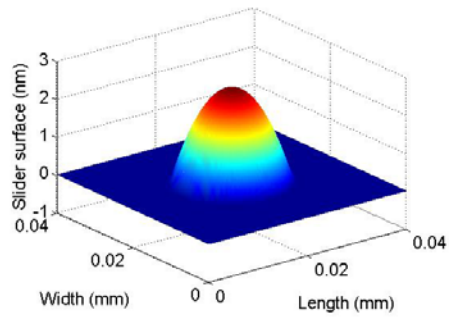


(b) Air bearing pressure profile along the ABS's center line using the FK model.

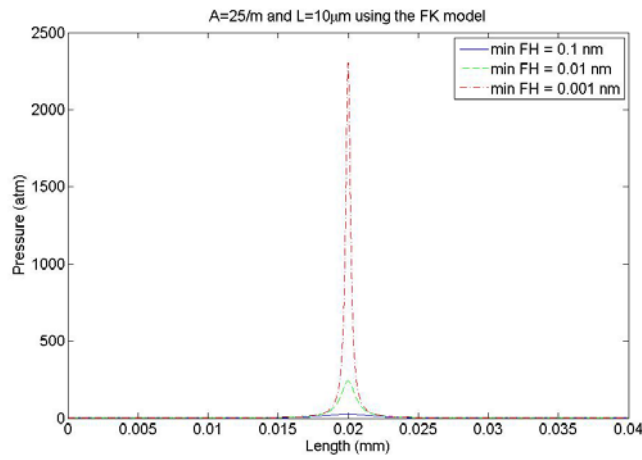


(c) Air bearing pressure profile along the ABS's center line using the pressure gradient model.

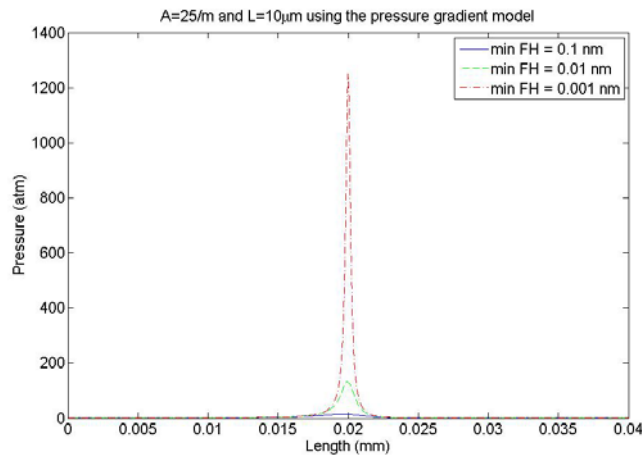
Fig. 6 ABS profile and air bearing pressure profile along the center line from the leading edge to the trailing edge in Case 2 ($A = 10^2$ /m and $L = 5 \mu\text{m}$).



(a) Air bearing surface profile

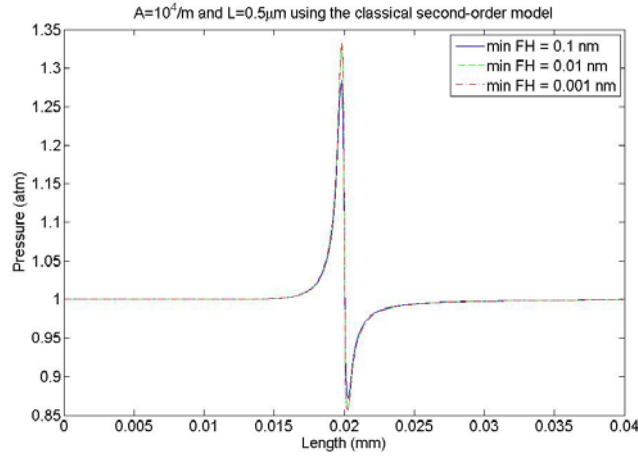


(b) Air bearing pressure profile along the ABS's center line using the FK model

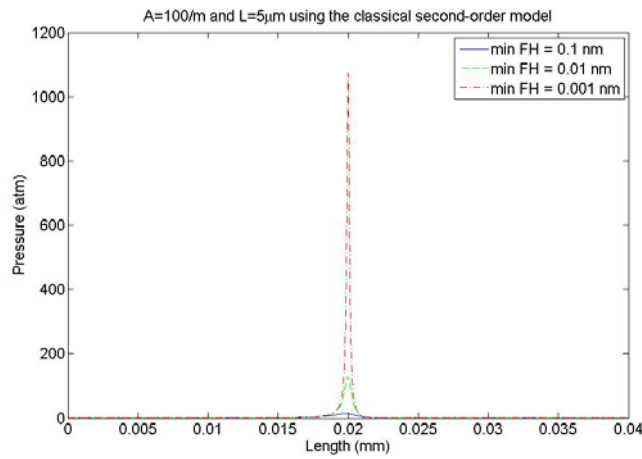


(c) Air bearing pressure profile along the ABS's center line using the pressure gradient model

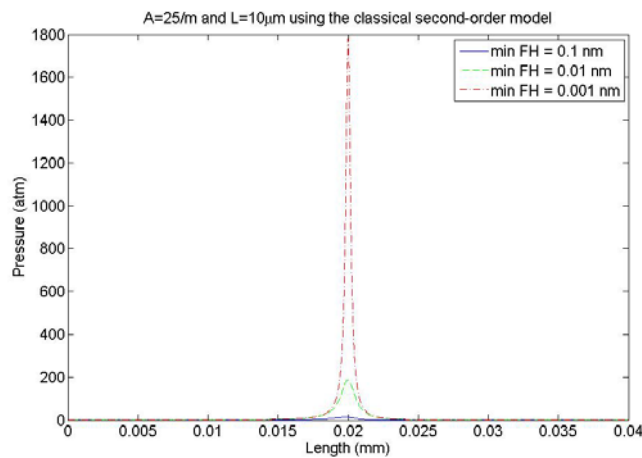
Fig. 7 ABS profile and air bearing pressure profile along the center line from the leading edge to the trailing edge in Case 3 ($A = 25 / \text{m}$ and $L = 10 \mu\text{m}$).



(a) Case 1 ($A = 104 / \text{m}$ and $L = 0.5 \mu\text{m}$).



(b) Case 2 ($A = 102 / \text{m}$ and $L = 5 \mu\text{m}$).



(c) Case 3 ($A = 25 / \text{m}$ and $L = 10 \mu\text{m}$).

Fig. 8 Air bearing pressure profile along the center line from the leading edge to the trailing edge obtained using the classical second-order model.